International Journal of Heat and Mass Transfer 52 (2009) 2399–2406

Contents lists available at ScienceDirect

International Journal of Heat and Mass Transfer

journal homepage: www.elsevier.com/locate/ijhmt

# Heat and mass transfer for Soret and Dufour's effects on Hiemenz flow through porous medium onto a stretching surface

R. Tsai, J.S. Huang *

*Department of Mechanical Engineering, Chung Yuan Christian University, No. 200, Chungpei Rd., Taoyuan, Chung Li 32023, Taiwan*

ARTICLE INFO

*Article history:*
Received 21 February 2008
Received in revised form 10 October 2008
Available online 8 January 2009

*Keywords:*
Chemical reaction
Soret and Dufour's effects
Variable viscosity
Stretching surface
Porous medium
Thermal radiation

ABSTRACT

A theoretical study of the steady stagnation point flow over a flat stretching surface in the presence of species concentration and mass diffusion under Soret and Dufour's effects has been obtained by solving the governing equations of continuity, momentum, energy and concentration using similarity analysis and numerical technique. Results showed that the fields were influenced appreciably by the effects of exothermic or endothermic chemical reaction, stretching parameter and radiation, etc. It was evident that for some kinds of mixtures with the light and medium molecular weight, the Soret and Dufour's effects should be considered as well.



## 1. Introduction

The fluid flow phenomena through a porous medium is commonly seen in the daily life and widely used in many engineering applications. Many practical diffusive operations involve the molecular diffusion of species in the presence of a chemical reaction within or at the boundary layer. Usually, the chemical reactions include two types. A homogeneous reaction is one that occurs uniformly throughout a given phase. The species generation in a homogeneous reaction is analogous to internal source of heat generation. In contrast, a heterogeneous reaction takes place in a restricted region or within the boundary of a phase. It can therefore be treated as a boundary condition similar to the constant heat flux condition in heat transfer. The study of heat and mass transfer within a chemical reaction is of great practical importance to engineers and scientists because of its almost universal occurrence in many branches of science and engineering [1]. Hiemenz discovered that stagnation point flow can be analyzed using the Navier–Stokes equation for the flow field [2]. Later, the heat transfer of stagnation point flow was considered by Goldstein [3]. The temperature distributions were reported by Sibulkin [4]. Sakiadis [5] initiated the study of boundary layer flow over a continuous solid surface moving with a constant speed. Yih [6] studied the heat transfer phenomenon of magneto hydrodynamic Hiemenz flow under the effect of uniform suction/blowing through the porous medium. Acharya et al. [7] studied heat and mass transfer over an accelerating surface with a heat source in the presence of suction and blowing. Attia [8] studied a similar solution for the plane flow through porous medium onto a stretching surface with internal heat source for both the momentum and energy governing equations.

Chemical reactions usually accompany a large amount of exothermic and endothermic reactions. These characteristics can be easily seen in a lot of industrial processes. Recently, it has been realized that it is not always permissible to neglect the convection effects in porous constructed chemical reactors [9]. The reaction produced in a porous medium was extraordinarily in common, such as the topic of PEM fuel cells modules and the polluted underground water because of discharging the toxic substance, etc.

Fourier's law, for instance, described the relation between energy flux and temperature gradient. In other aspects, Fick's law was determined by the correlation of mass flux and concentration gradient. Moreover, it was found that energy flux can also be generated by composition gradients, pressure gradients, or body forces. The energy flux caused by a composition gradient was discovered in 1873 by Dufour and was correspondingly referred to the Dufour effect. It was also called the diffusion-thermo effect. On the other hand, mass flux can also be created by a temperature gradient, as was established by Soret. This is the thermal-diffusion effect. In general, the thermal-diffusion and the diffusion-thermo effects were of a smaller order of magnitude than the effects described by Fourier's or Fick's law and were often neglected in heat and mass transfer processes. There were still some exceptional conditions. The thermal-diffusion effect has been utilized for isotope separation and in

* Corresponding author. Tel.: +886 3 2654324; fax: +886 3 2654399.
*E-mail address:* lilysonq@yahoo.com.tw (J.S. Huang).

0017-9310/$ - see front matter © 2008 Elsevier Ltd. All rights reserved.
doi:10.1016/j.ijheatmasstransfer.2008.10.017

**Nomenclature**

| | |
|---|---|
| $a$ | free stream strength |
| $C$ | concentration |
| $C_f$ | skin friction coefficient |
| $c$ | characteristic stretching coefficient |
| $c_p$ | specific heat capacity at constant pressure |
| $c_s$ | concentration susceptibility |
| $c_1$,$c_2$ | positive constant |
| $D_e$ | effective mass diffusivity |
| $D_f$ | Dufour number |
| $e$ | natural exponent |
| $f$ | dimensionless flow stream function |
| $G$ | temperature buoyancy parameter |
| $g$ | acceleration due to gravity |
| $J$ | mass flux |
| $K$ | permeability |
| $k_e$ | effective thermal conductivity |
| $k_T$ | thermal-diffusion ratio |
| $k^*$ | Rosseland mean absorption coefficient |
| $k_1$ | rate of chemical reaction |
| $L$ | power index |
| $Le$ | Lewis number |
| $M$ | magnetic parameter |
| $N$ | concentration buoyancy parameter |
| $Nu$ | Nusselt number |
| Pr | Prandtl number |
| $Q$ | volumetric rate of heat generation/absorption |
| $q$ | heat flux |
| $q_r$ | radiative heat flux |
| $R$ | radiation parameter |
| Re | Reynolds number |
| $S$ | stretching parameter |
| $Sh$ | Sherwood number |
| $S_r$ | Soret number |
| $T$ | temperature |
| $T_m$ | mean fluid temperature |
| $(U,V)$ | the velocity components for the potential flow |
| $(u,v)$ | components for the potential flow of velocity at any point $(x, y)$ |
| $v_0$ | wall suction/injection velocity |
| $(x,y)$ | cartesian coordinates |

*Greek symbols*

| | |
|---|---|
| $\alpha$ | viscosity parameter |
| $\alpha_e$ | effective thermal diffusivity |
| $\beta_T$ | thermal expansion coefficient |
| $\beta_C$ | concentration expansion coefficient |
| $\gamma$ | chemical reaction parameter |
| $\delta$ | heat source parameter |
| $\eta$ | similarity parameter |
| $\theta$ | dimensionless temperature |
| $\lambda$ | power index |
| $\mu$ | dynamic viscosity |
| $\mu_0$ | viscosity at wall temperature |
| $\nu$ | kinematic viscosity |
| $\rho$ | fluid density |
| $\sigma^*$ | Stefan–Boltzman constant |
| $\tau$ | shear stress |
| $\phi$ | dimensionless concentration |
| $\psi$ | stream function |
| $\Omega$ | porosity parameter |

*Subscripts*

| | |
|---|---|
| $\infty$ | free stream condition |
| max | maximum |
| $w$ | surface condition |

mixtures between gases with very light molecular weight ($H_2$, $He$) and of medium molecular weight ($N_2$, air), the diffusion-thermo effect was found to be of a magnitude such that it may not be neglected in certain conditions [10]. In recent years, Kandasamy et al. studied the heat and mass transfer under a chemical reaction with a heat source [1,11]. Seddeek studied the thermal radiation and buoyancy effect on MHD free convection heat generation flow over an accelerating permeable surface with the influence temperature dependent viscosity [12], and later the chemical reaction, variable viscosity, radiation, variable suction on hydromagnetic convection flow problems were included [13–15]. Liao and Pop [16] offered an entirely research about the boundary layer flow over a flat plate embedded in a porous medium. Chamkha and Ben-Nakhi [17] who analyzed the MHD mixed convection flow under the radiation interaction along a vertical permeable surface immersed in a porous medium in the presence of Soret and Dufour's effects.

Although there are numerous widely practical applications in industrial processes, few previous published papers discussed the combined relation. In the present work we focus mainly on the heat and mass transfer under a chemical reaction, heat source, radiation, stretching surface and variable viscosity coupled with the Soret and Dufour's effects which occur in a porous medium for the Hiemenz flow.

## 2. Mathematical formulation

Consider the two-dimensional, steady state, viscous laminar Hiemenz flow through a porous medium onto a vertical flat stretching surface. The viscosity of the fluid varies with the natural exponent and is expressed in the form $\mu/\mu_0 = e^{-\alpha\theta}$ [18] and $\mu_0$ is the viscosity at temperature $T_w$ and $\alpha$ is the viscosity parameter. The heat generation or absorption and its property variations due to temperature are limited to density and viscosity. The density variation and the buoyancy effect are taken into consideration which could be adopted the Boussinesq approximations for both the temperature and concentration gradient. In addition, the Joule heating is neglected but the radiation, Soret and Dufour's effects are examined. The chemical reaction is taking place in the flow over the porous medium with the effective mass diffusivity $D_e$ and the rate of chemical reaction $k_1$ throughout the fluid. As shown in Fig. 1, $x$-axis is along the direction of plate and $y$-axis normal to it. The $u$, $v$ are the velocity of $x$ and $y$ component, $T$ and $C$ are the temperature and concentration, respectively. Under these assumptions, the governing boundary layer equations of momentum, energy and diffusion under Boussinesq approximations could be written as follows:

$$\frac{\partial u}{\partial x}+\frac{\partial v}{\partial y}=0 \tag{1}$$

$$u\frac{\partial u}{\partial x}+v\frac{\partial u}{\partial y}=\frac{1}{\rho}\frac{\partial}{\partial y}\left(\mu\frac{\partial u}{\partial y}\right)+U_\infty\frac{dU_\infty}{dx}-\frac{v}{K}(u-U_\infty)+g[\beta_T(T-T_\infty)+\beta_C(C-C_\infty)] \tag{2}$$

$$u\frac{\partial T}{\partial x}+v\frac{\partial T}{\partial y}=\alpha_e\frac{\partial^2 T}{\partial y^2}-\frac{1}{\rho c_p}\frac{\partial q_r}{\partial y}+\frac{Q}{\rho c_p}(T-T_\infty)+\frac{D_e k_T}{c_s c_p}\frac{\partial^2 C}{\partial y^2} \tag{3}$$

$$u\frac{\partial C}{\partial x}+v\frac{\partial C}{\partial y}=D_e\frac{\partial^2 C}{\partial y^2}-k_1 C+\frac{D_e k_T}{T_m}\frac{\partial^2 T}{\partial y^2} \tag{4}$$

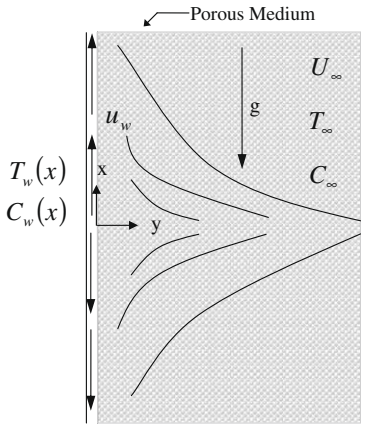


**Fig. 1.** Stagnation point flow model schematic.

The boundary conditions are given by

$$y = 0; \quad u = u_w = cx, \quad v = 0, \quad T = T_w, \quad C = C_w \tag{5a}$$

$$y \to \infty; \quad u = U_\infty = ax, \quad T = T_\infty, \quad C = C_\infty \tag{5b}$$

Both the wall temperature and concentration are assumed to express as the power-law variation forms

$$T_w = T_\infty + c_1 x^L, \quad C_w = C_\infty + c_2 x^L \tag{6}$$

where $c_1$ and $c_2$ are constant and $L$ is the power index of the wall temperature and concentration, $c$ and $a$ are the positive constants that represent the characteristic stretching intensity and the free stream strength. $\rho$, $\mu$, and $c_p$ are the density, dynamic viscosity and the specific heat at constant pressure, respectively. $K$ is the permeability of the porous medium, $g$ is the gravitational acceleration, $\beta_T$ and $\beta_C$ are the expansion coefficients of temperature and concentration. $U$, $T$ and $C$ are the flow velocity, temperature and concentration, separately. The subscripts $w$ and $\infty$ stand for the wall and free stream conditions. $k_e$ as well as $\alpha_e (= k_e/\rho c_p)$ are the effective thermal conductivity and diffusivity of the porous medium, $Q$ is the volumetric heat generation/absorption rate. $k_T$, $c_s$, $T_m$ and $q_r$ are the thermal-diffusion ratio, concentration susceptibility, fluid mean temperature and the radiative heat flux, respectively. Using the Rosseland approximation (Sparrow and Cess [19], and EL-A rabawy [20]), the radiative heat flux $q_r$ could be expressed by

$$q_r = -\frac{4\sigma^*}{3k^*}\frac{\partial T^4}{\partial y} \tag{7}$$

where the $\sigma^*$ represents the Stefan–Boltzman constant and $k^*$ is the Rosseland mean absorption coefficient. If assuming that the temperature difference within the flow are sufficiently small such that $T^4$ could be approached as the linear function of temperature

$$T^4 \cong 4T_\infty^3 T - 3T_\infty^4 \tag{8}$$

The equation of continuity is satisfied if we choose a stream function $\psi(x, y)$ such that $u = \frac{\partial \psi}{\partial y}$ and $v = -\frac{\partial \psi}{\partial x}$. The governing partial differential equations (1)–(4) admit similarity solutions for obtaining the dimensionless stream function $f(\eta)$, temperature $\theta(\eta)$, and concentration $\phi(\eta)$. The relative parameters are introduced as

$$\psi = \sqrt{cv}xf(\eta), \quad u = cxf'(\eta), \quad v = -\sqrt{cv}f(\eta), \quad \eta = \sqrt{\frac{c}{v}}y,$$

$$\theta(\eta) = \frac{T - T_\infty}{T_w - T_\infty}, \quad \phi(\eta) = \frac{C - C_\infty}{C_w - C_\infty}$$

After introducing the similarity transformation, the equations of (2)–(4) can be transformed into a set of following forms in terms with $f(\eta)$, $\theta(\eta)$ and $\phi(\eta)$ could be expressed as

$$f''' + e^{\alpha\theta}[ff'' - (f')^2 + S^2] - \alpha\theta' f'' + G\theta e^{\alpha\theta} + N\phi e^{\alpha\theta} + \Omega e^{\alpha\theta}(S - f') = 0 \tag{9}$$

$$\left(\frac{R+1}{R}\right)\theta'' + \Pr(f\theta' - Lf'\theta + \delta\theta) + D_f\phi'' = 0 \tag{10}$$

$$\phi'' + \Pr Le(f\phi' - Lf'\phi - \gamma\phi) + S_r Le\theta'' = 0 \tag{11}$$

where the prime denotes a partial differentiation with respect to $\eta$. The transformed boundary conditions are given by

$$\eta = 0; \quad f(0) = 0, \quad f'(0) = 1, \quad \theta(0) = 1, \quad \phi(0) = 1 \tag{12a}$$

$$\eta \to \eta_\infty; \quad f'(\infty) = S, \quad \theta(\infty) = 0, \quad \phi(\infty) = 0 \tag{12b}$$

**Table 1**
Comparison of the values $NuPe^{-1/2}$ with Pr = 1.0, $Le$ = 1.0, $\alpha$ = 0.0, $\gamma$ = 0.6, $R = 10^9$, $M$ = 0.0, $\delta$ = 0.0, $G$ = 0.0, $N$ = 0.0, $v_0$ = 0.0.

| $\Omega$ | Yih [6] | Chamkha and Khaled [21] | Seddeek et al. [13] | Present study |
|---|---|---|---|---|
| | $L = \lambda = 0$ | | | |
| 0 | 0.570465 | 0.570465 | 0.570465 | 0.570428 |
| 0.0001 | 0.570468 | 0.572804 | 0.570464 | 0.570432 |
| 0.001 | 0.570497 | 0.572833 | 0.570493 | 0.570460 |
| 0.01 | 0.570782 | 0.573120 | 0.570780 | 0.570746 |
| 0.1 | 0.573556 | 0.575904 | 0.573551 | 0.573523 |
| 1 | 0.595346 | 0.597787 | 0.595344 | 0.595330 |
| | $L = \lambda = 1$ | | | |
| 0 | 0.811301 | 0.815499 | 0.811381 | 0.811262 |
| 0.0001 | 0.811307 | 0.812658 | 0.811391 | 0.811268 |
| 0.001 | 0.811355 | 0.812706 | 0.811359 | 0.811316 |
| 0.01 | 0.811833 | 0.813185 | 0.811841 | 0.811795 |
| 0.1 | 0.816490 | 0.817842 | 0.816495 | 0.816455 |
| 1 | 0.853324 | 0.854695 | 0.853331 | 0.853306 |

**Table 2**
Comparison of the values $NuRe^{-1/2}$ with $Le$ = 1.0, $\alpha$ = 0.0, $\gamma$ = 0.6, $R = 10^9$, $M$ = 0.0, $\Omega$ = 0.0, $\delta$ = 0.0, $G$ = 0.0, $N$ = 0.0, $v_0$ = 0.0.

| Pr | Yih [6] | Chamkha and Khaled [21] | Seddeek et al. [13] | Present study |
|---|---|---|---|---|
| | $L = \lambda = 0$ | | | |
| 1 | 0.570465 | 0.577689 | 0.570467 | 0.570428 |
| 10 | 1.338796 | 1.354430 | 1.339442 | 1.339367 |
| | $L = \lambda = 1$ | | | |
| 1 | 0.811301 | 0.815499 | 0.811381 | 0.811262 |
| 10 | 1.861577 | 1.870514 | 1.862408 | 1.862357 |

**Table 3**
Comparison of the values $f''(0)$ with Pr = 1.0, $Le$ = 1.0, $\alpha$ = 0.0, $\gamma$ = 0.6, $R = 10^3$, $\Omega$ = 0.0, $L$ = 0.0 $\delta$ = 0.0, $G$ = 0.0, $N$ = 0.0.

| $M$ | Yih [6] | Chamkha and Khaled [21] | Seddeek et al. [13] | Present study |
|---|---|---|---|---|
| | $v_0 = -1$ | | | |
| 0 | 0.75658 | 0.75689 | 0.75659 | 0.75650 |
| 1 | 1.11642 | 1.11634 | 1.11644 | 1.11636 |
| 4 | 1.87762 | 1.87633 | 1.87766 | 1.87759 |
| | $v_0 = 0$ | | | |
| 0 | 1.23259 | 1.23290 | 1.23257 | 1.23253 |
| 1 | 1.58533 | 1.58494 | 1.58530 | 1.58531 |
| 4 | 2.34666 | 2.34457 | 2.34662 | 2.34665 |
| | $v_0 = 1$ | | | |
| 0 | 1.88931 | 1.88890 | 1.88933 | 1.88922 |
| 1 | 2.20294 | 2.20164 | 2.20295 | 2.20289 |
| 4 | 2.92011 | 2.91669 | 2.92013 | 2.92009 |

where $\Omega(=\nu/cK)$ is the porosity parameter, $S(=a/c)$ is the stretching parameter, $G(=g\beta_T(T_w-T_\infty)/cu_w)$ and $N(=g\beta_C(C_w-C_\infty)/cu_w)$ represent the temperature and concentration buoyancy parameters, respectively. Pr is Prandtl number, $Le$ is Lewis number, $R(=3k^*k_e/16\sigma^*T_\infty^3)$ is the radiation parameter and $\delta(=Q/c\rho c_p)$ is the heat source parameter. $\gamma(=k_1/c)$ represents the chemical reaction parameter, $D_f(=D_ek_T(C_w-C_\infty)/c_sc_p(T_w-T_\infty))$ and $S_r(=D_ek_T\ (T_w-T_\infty)/T_m\alpha_e(C_w-C_\infty))$ stand for the Dufour and Soret numbers.

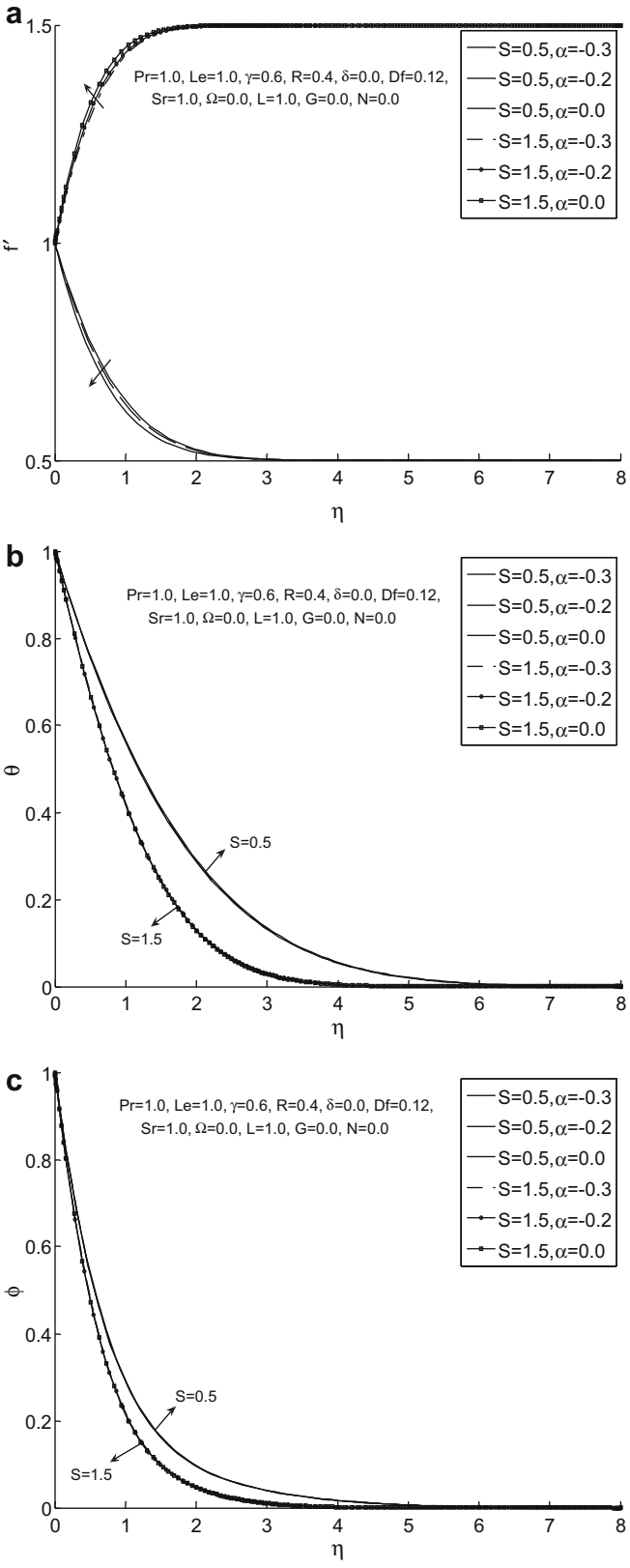


**Fig. 2.** Effect of viscosity parameter on the velocity, temperature and concentration profiles under Soret and Dufour's effects.

Of special significance for the flow, heat and mass transfer situation are the skin-friction coefficient $C_f$, local Nusselt number $Nu$, and Sherwood number $Sh$. These physical quantities could be defined as

$$\tau_w=\mu\left(\frac{\partial u}{\partial y}\right)_{y=0};\quad C_f=\frac{1}{(1/2)\rho u_w^2}=2f''(0)\mathrm{Re}^{-1/2} \tag{13}$$

$$q_w=-k_e\left(\frac{\partial T}{\partial y}\right)_{y=0};\quad Nu=\frac{xq_w}{k_e(T_w-T_\infty)}=-\theta'(0)\mathrm{Re}^{1/2} \tag{14}$$

$$J_w=-D_e\left(\frac{\partial C}{\partial y}\right)_{y=0};\quad Sh=\frac{J_wx}{D_e(C_w-C_\infty)}=-\phi'(0)\mathrm{Re}^{1/2} \tag{15}$$

where $q_w$ and $J_w$ are the wall heat and mass flux, respectively. Re = $u_wx/\nu$ is the local Reynolds number.

The set of non-linear ordinary Eqs. (9)–(11) with boundary conditions (12) have been solved using the fourth order of Runge–Kutta integration accompanied with the shooting scheme. The grid mesh of $\Delta\eta=0.01$ is selected to be satisfactory for a convergence criterion of $10^{-6}$ in nearly all cases and the maximum values of $\eta_{\max}=8.0$ which is sufficient large for the velocity to approach the relevant stream velocity. In order to check the method of numerical accuracy, Tables 1–3 are the data comparisons with the previous published papers and the results are found in good agreement.

## 3. Results and discussion

In order to gain physical insight the velocity, temperature and concentration have been discussed by assigning numerical values to the parameter encounter in the problem which the numerical results are tabulated and displayed with the graphical illustrations.

Fig. 2 represent the velocity, temperature and concentration profiles, respectively. The parameter $S$ stands for the ratio of free stream strength compared to the stretching intensity. Under the constant speed of stretching velocity, the increasing $S$ coincides with the enhancement of the free stream velocity and the curves could be seen in Fig. 2(a). The stronger free stream velocity would lead to the thinner thermal and diffusion boundary layers as shown in Fig. 2(b) and (c). The influence is shown in Table 4. Moreover, from the profiles we can realize that the viscosity parameter plays just a tiny role for the flow, energy and diffusion fields, the mainly effect which influences the whole fields are the stretching parameter but it still could be found a little change with the various $\alpha$. Fig. 3 displays the velocity, temperature and concentration profiles under the different buoyancy ratio at $S=0.5$. The increasing buoyancy parameter indicates the larger temperature and concentration gradient from the wall relative to the ambient. In other words, the gradually increasing $G$ and $N$ coincide with the stronger buoyancy force and thus lead to the larger velocity. The larger velocity accompanies with the decreasing boundary layer thickness of thermal and

**Table 4**
Numerical values of local skin-friction coefficient, Nusselt and Sherwood number for Pr = 1.0, $Le$ = 1.0, $\alpha$ = 0.0, $\gamma$ = 0.6, $R$ = 0.4, $\Omega$ = 0.0, $L$ = 1.0, $\delta$ = 0.0, $G$ = 0.0, $N$ = 0.0 under stretching effect.

| $S$ | $C_f\mathrm{Re}^{1/2}/2$ | $Nu\mathrm{Re}^{-1/2}$ | $Sh\mathrm{Re}^{-1/2}$ |
|---|---|---|---|
| 0.5 | −0.6673 | 0.5368 | 1.2109 |
| 1.0 | 0.0000 | 0.6403 | 1.2858 |
| 1.5 | 0.9095 | 0.7282 | 1.3653 |

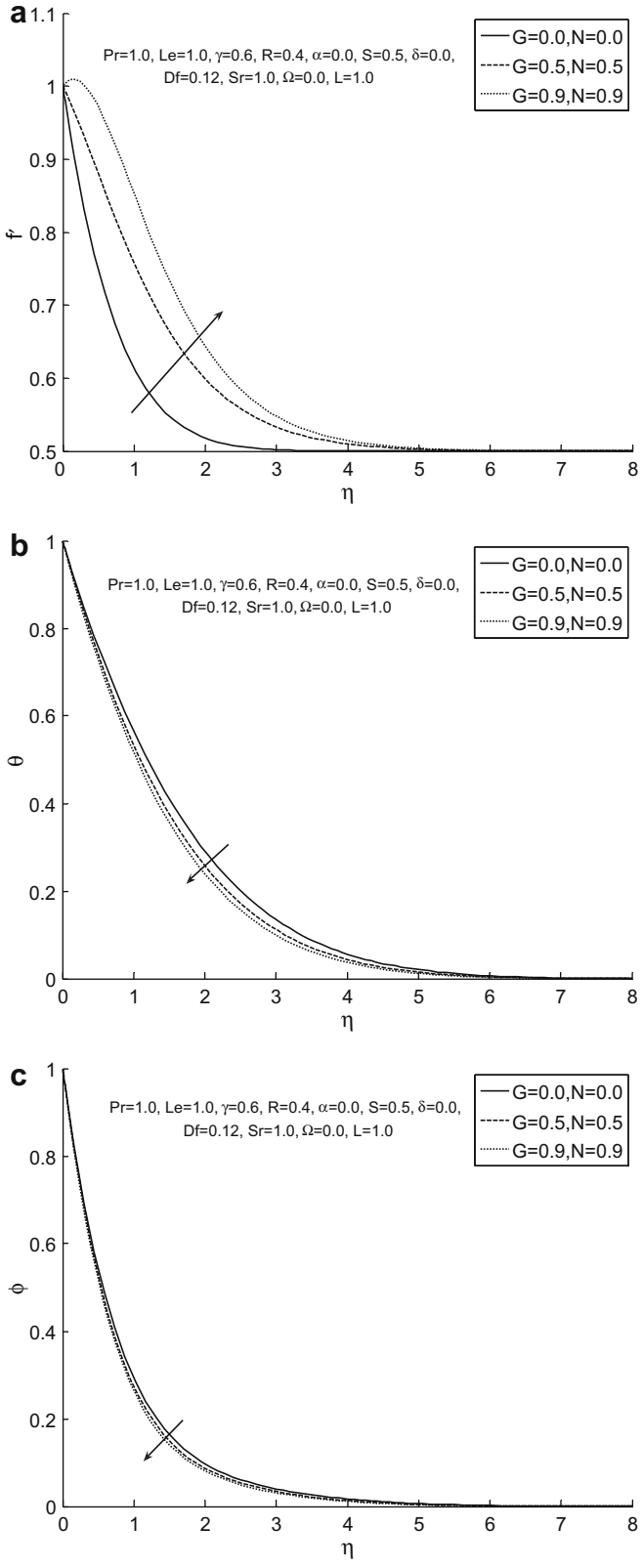


**Fig. 3.** Effect of buoyancy parameter on the velocity, temperature and concentration profiles under Soret and Dufour's effects.

concentration. Fig. 4 shows the dimensionless temperature decreases with increasing radiation parameter. The physical facts could be explained by the effect of radiation $(1/R)$ is to increase the flux of energy transport to the fluid and accordingly increase

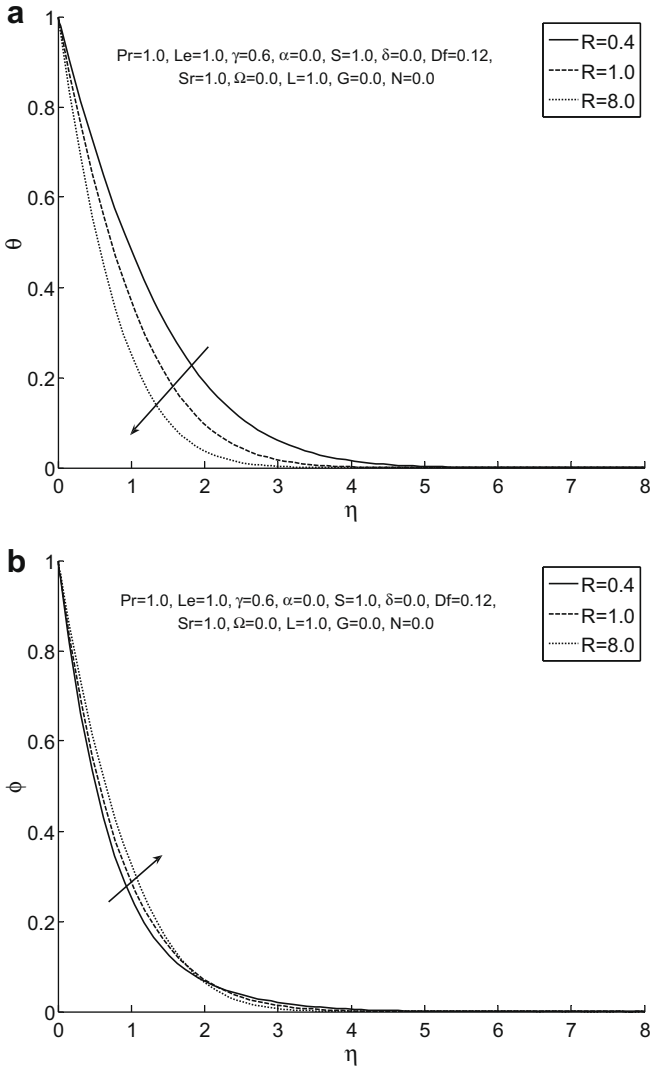


**Fig. 4.** Effect of radiation parameter on the temperature and concentration profiles under Soret and Dufour's effects.

the fluid temperature. In addition, as $R$ decreases, the concentration gradient becomes steeper. The Prandtl number effect on the temperature and concentration are plotted on the profiles for Fig. 5. Generally, the selected Prandtl number is considered to characterize for gases or liquid mixtures. The boundary layer thickness decreases with the increasing Prandtl number in both temperature and concentration fields. Based on the physical point of view, for the given viscosity, while the bigger Prandtl number which coincides with the weaker thermal diffusivity and thinner boundary layer. The parameter $\delta$ stands for the heat generation or absorption rate. The positive sign indicates the generation whereas negative means absorption. From the Fig. 6 we could realize that the increasing heat source parameter follows with the stronger heat generation and the increasing thermal boundary layer, but the influence on the diffusion boundary layer is relative small. Figs. 7 and 8 introduce the chemical reaction and various Lewis number effects on the concentration profiles. The bigger reaction parameter accompanies with severe reaction condition and thus results in the steeper curves of diffusion boundary layer. For the same thermal diffusivity, as $Le$ gradually increases, this corresponds to the weaker molecular diffusivity and the thinner boundary layer thickness. The Soret and Dufour's effects could be apparently seen in Fig. 9. From the Soret number definition, which represents the ratio of temperature

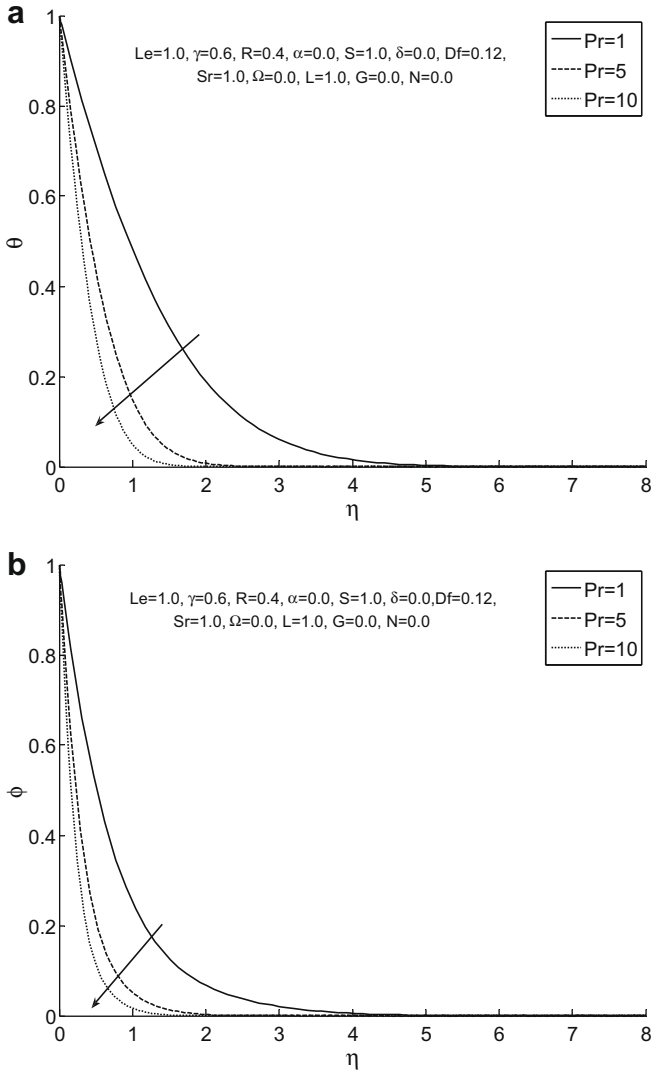


**Fig. 5.** Effect of Prandtl number on the temperature and concentration profiles under Soret and Dufour's effects.

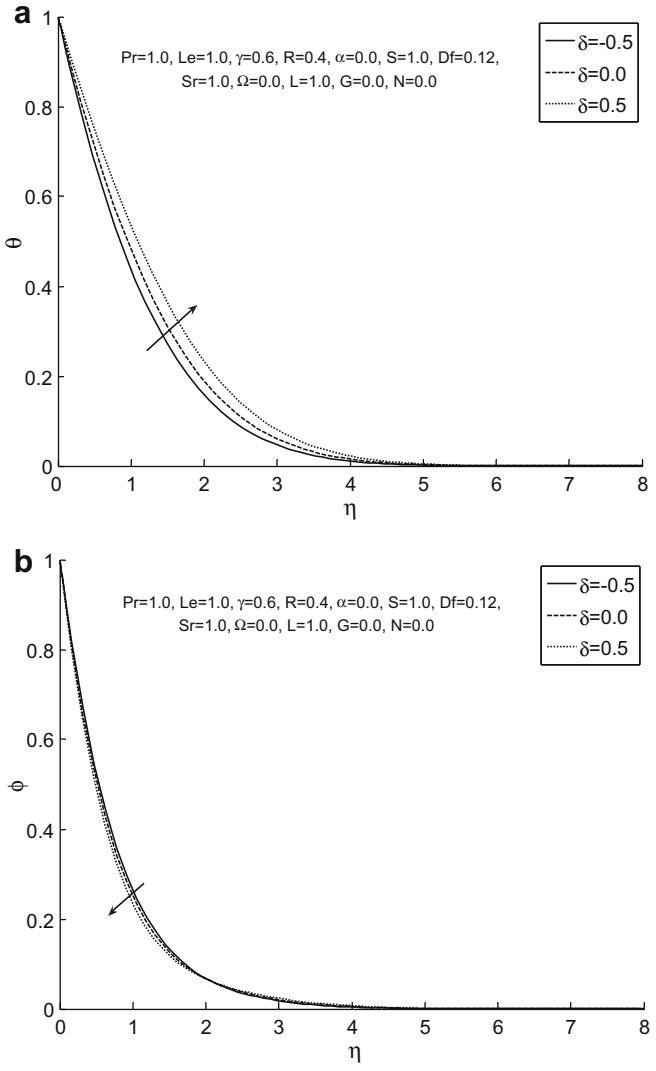


**Fig. 6.** Effect of heat source parameter on the temperature and concentration profiles under Soret and Dufour's effects.

difference compared to the concentration, the Dufour number is opposite. Hence, the bigger Soret number stands for a larger temperature difference and precipitous gradient. On the other hand, the Dufour number symbolizes the same meaning in mass transfer. Furthermore, the Soret and Dufour number effects on the temperature field could be observed in Fig. 9(a). We observe that quantitatively, when $\eta = 1.0$ and $S_r$ decreases from 2.0 to 1.0 there is 1.69% increase in the temperature value, whereas the corresponding increase is 6.87%, when $S_r$ decreases from 0.5 to 0.1. The Soret and Dufour number effects on the concentration field are displayed in Fig. 9(b). Quantitatively, when $\eta = 1.0$ and $S_r$ decreases from 2.0 to 1.0 there is 25.89% decrease in the concentration value, whereas the corresponding decrease is 15.31%, when $S_r$ decreases from 0.5 to 0.1. Table 5 shows the data of heat and mass transfer rate. From the table, we could determine that as the Soret number decreases and the Dufour number increases, this corresponds to a weakened heat transfer rate and enhanced mass transfer rate. Tables 6 and 7 symbolize the chemical reaction which occurs in the porous medium with the exothermic and endothermic reaction. The heat transfer rate decreases with the heat generation but increases with heat absorption. Conversely, the mass transfer rate shows opposite results that match with the proposal by Soret and Dufour.

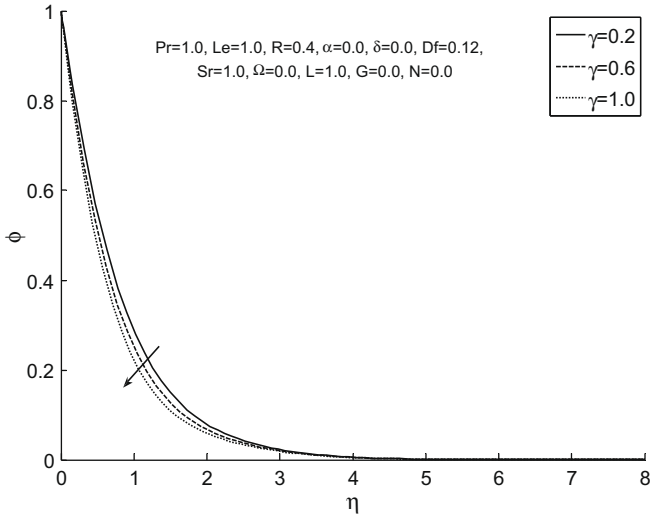


**Fig. 7.** Effect of chemical reaction parameter on the concentration profiles under Soret and Dufour's effects.

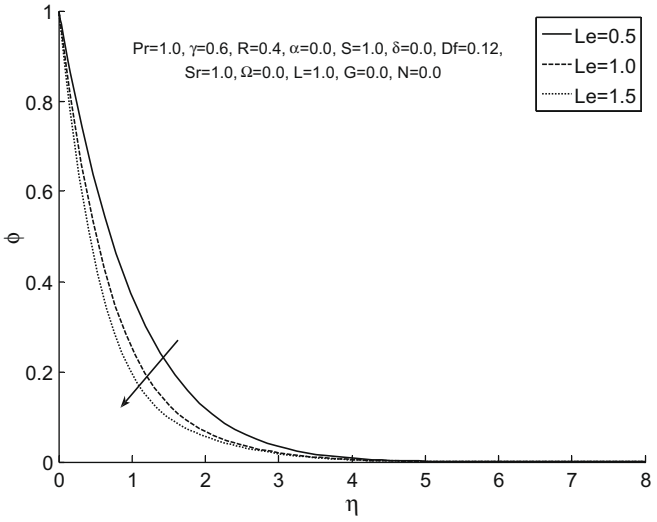


**Fig. 8.** Effect of Lewis number on the concentration profiles under Soret and Dufour's effects.

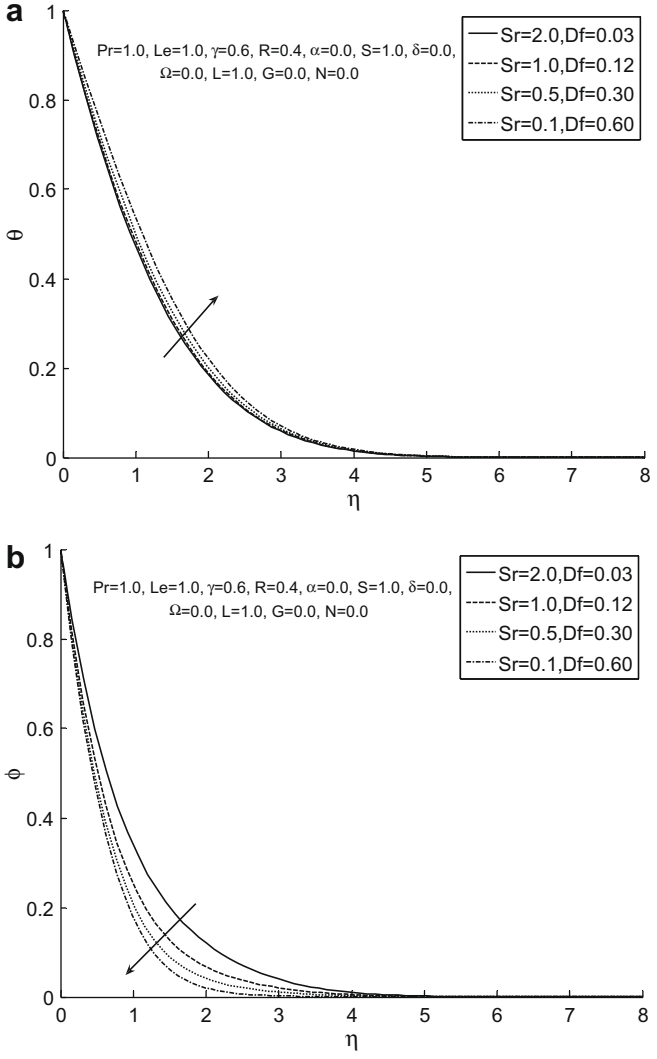


**Fig. 9.** Effect of Soret and Dufour numbers on the temperature and concentration profiles.

**Table 5**
Numerical values of local Nusselt and Sherwood number for Pr = 1.0, $Le$ = 1.0, $\alpha$ = 0.0, $\gamma$ = 0.6, $R$ = 0.4, $\Omega$ = 1.0, $L$ = 1.0, $\delta$ = 0.0, $G$ = 0.0, $N$ = 0.0, $S$ = 1.0 under Soret and Dufour's effects.

| $S_r$ | $D_f$ | $Nu\mathrm{Re}^{-1/2}$ | $Sh\mathrm{Re}^{-1/2}$ |
|---|---|---|---|
| 2.0 | 0.03 | 0.6641 | 1.0726 |
| 1.0 | 0.12 | 0.6403 | 1.2858 |
| 0.5 | 0.30 | 0.5881 | 1.3941 |
| 0.1 | 0.60 | 0.4972 | 1.4589 |

**Table 6**
Numerical values of local Nusselt and Sherwood number for Pr = 1.0, $Le$ = 1.0, $\alpha$ = 0.0, $\gamma$ = 0.6, $R$ = 0.4, $\Omega$ = 1.0, $L$ = 1.0, $\delta$ = 0.5, $G$ = 0.0, $N$ = 0.0, $S$ = 1.0 under Soret and Dufour's effects.

| $S_r$ | $D_f$ | $Nu\mathrm{Re}^{-1/2}$ | $Sh\mathrm{Re}^{-1/2}$ |
|---|---|---|---|
| 2.0 | 0.03 | 0.5518 | 1.2070 |
| 1.0 | 0.12 | 0.5254 | 1.3545 |
| 0.5 | 0.30 | 0.4695 | 1.4293 |
| 0.1 | 0.60 | 0.3749 | 1.4661 |

**Table 7**
Numerical values of local Nusselt and Sherwood number for Pr = 1.0, $Le$ = 1.0, $\alpha$ = 0.0, $\gamma$ = 0.6, $R$ = 0.4, $\Omega$ = 1.0, $L$ = 1.0, $\delta$ = -0.5, $G$ = 0.0, $N$ = 0.0, $S$ = 1.0 under Soret and Dufour's effects.

| $S_r$ | $D_f$ | $Nu\mathrm{Re}^{-1/2}$ | $Sh\mathrm{Re}^{-1/2}$ |
|---|---|---|---|
| 2.0 | 0.03 | 0.7619 | 0.9499 |
| 1.0 | 0.12 | 0.7403 | 1.2231 |
| 0.5 | 0.30 | 0.6911 | 1.3620 |
| 0.1 | 0.60 | 0.6030 | 1.4524 |

## 4. Conclusions

This work studied the Soret and Dufour's effects on Hiemenz flow through the porous medium onto a stretching surface. The buoyancy force, variable viscosity, radiation, heat generation/absorption and chemical reaction effects were considered in the separate cases. From the obtained results, we realize that under the combined effects, which correlate to the flow trend, the thermal and diffusion boundary layer thickness includes the Soret and Dufour's effects. In addition, the present analysis also shows the self-evident influence in the relation of temperature and concentration fields from the profiles. From the above analysis we conclude that for some kinds of mixtures (for example, $H_2$-air) with the light and medium molecular weight, the Soret and Dufour's effects play a significant role and should be taken into consideration as well.

## References

[1] R. Kandasamy, K. Periasamy, K.K. Sivagnana Prabhu, Chemical reaction, heat and mass transfer on MHD flow over a vertical stretching surface with heat source and thermal stratification effects, Int. J. Heat Mass Transfer 48 (2005) 4557–4561.
[2] F.M. White, Viscous Fluid Flow, second ed., McGraw-Hill, New York, 1991.
[3] S. Goldstein, Modern Developments in Fluid Dynamics, Clarendon Press, Oxford, 1938.
[4] M. Sibulkin, Heat transfer at the rear and forward stagnation points of a body of revolution, J. Aeronaut. Sci. 19 (1952) 570–577.
[5] B.C. Sakiadis, Boundary layer behavior on continuous solid surfaces: I. Boundary layer equations for two-dimensional and axisymmetric flow, AIChE J. 7 (1) (1961) 26–28.
[6] K.A. Yih, The effect of uniform suction/ blowing on heat transfer of magnetohydrodynamic Hiemenz flow through porous media, Acta Mech. 130 (1998) 147–158.
[7] M. Acharya, L.P. Singh, G.C. Dash, Heat and mass transfer on an accelerating surface subjected to both power law surface temperature and power law heat flux variations with temperature dependent heat source in the presence of suction and injection, Int. J. Eng. Sci. 37 (1999) 189–211.

[8] H.A. Attia, On the effectiveness of porosity on stagnation point flow towards a stretching surface with heat generation, Comput. Mater. Sci. 38 (2007) 741–745.
[9] D.A. Nield, A. Bejan, Convection in Porous Media, second ed., Springer-Verlag, New York, 1999.
[10] E.R.G. Eckert, R.M. Drake, Analysis of Heat and Mass Transfer, McGraw-Hill, New York, 1972.
[11] R. Kandasamy, K. Periasamy, K.K. Sivagnana Prabhu, Effect of chemical reaction, heat and mass transfer along a wedge with heat source and concentration in the presence of suction or injection, Int. J. Heat Mass Transfer 48 (2005) 1388–1394.
[12] M.A. Seddeek, Thermal radiation and buoyancy effects on MHD free convection heat generation flow over an accelerating permeable surface with temperature dependent viscosity, Can. J. Phys. 79 (2001) 725–732.
[13] M.A. Seddeek, A.A. Darwish, M.S. Abdelmeguid, Effect of chemical reaction and variable viscosity on hydromagnetic mixed convection heat and mass transfer for Hiemenz flow through porous media with radiation, Commun. Nonlinear Sci. Numer. Simul. 12 (2007) 195–213.
[14] M.A. Seddeek, A.M. Salem, The effect of an axial magnetic field on the flow and heat transfer about a fluid underlying the axisymmetric spreading surface with temperature dependent viscosity and thermal diffusivity, Comput. Mech. 39 (2007) 401–408.
[15] M.A. Seddeek, Faiza A. Salama, The effects of temperature dependent viscosity and thermal conductivity on unsteady MHD convective heat transfer past a semi-infinite vertical porous moving plate with variable suction, Comput. Mater. Sci. 40 (2007) 186–192.
[16] S.J. Liao, I. Pop, Explicit analytic solution for similarity boundary-layer equations, Int. J. Heat Mass Transfer 47 (2004) 75–85.
[17] A.J. Chamkha, A. Ben-Nakhi, MHD Mixed convection-radiation interaction along a permeable surface immersed in a porous medium in the presence of Soret and Dufour's Effect, Heat Mass Transfer 44 (2008) 845–856.
[18] E.M.A. Elbashbeshy, F.N. Ibrahim, Steady free convection flow with variable viscosity and thermal diffusivity along a vertical plate, J. Phys. D: Appl. Phys. 26 (1993) 2137–2143.
[19] E.M. Sparrow, R.D. Cess, Radiation Heat Transfer, Brooks/Cole, Belmont, California, 1970.
[20] H.A.M. El-Arabawy, Effect of suction/injection on the flow of a micropolar fluid past a continuously moving plate in the presence of radiation, Int. J. Heat Mass Transfer 46 (2003) 1471–1477.
[21] A.J. Chamkha, A.A. Khaled, Similarity solutions for hydromagnetic mixed convection heat and mass transfer for Hiemenz flow through porous media, Int. J. Numer. Meth. Heat Fluid Flow 10 (1) (2000) 94–115.